

Article Info

Accepted: 30/09/2021

Corresponding Author: * mgroumpos@gmail.com

DOI: <https://doi.org/10.48088/ejg.m.gro.12.2.20.35>

Research Article

The krathis lake, one century of evolution.

Maria **GROUMPOU**^{1*}, Pavlos **AVRAMIDIS**¹,
George **ILIOPOULOS**¹, Helen **PAPAEFTHYMIU**¹ &
Ioannis **K. KOUKOUVELAS**¹

¹ University of Patras, Greece

Keywords

*Landslides,
Ephemeral lakes,
Natural dams,
ICHGS-2019*

Abstract

A riverbed swamp in the Krathis River, N. Peloponnese, is studied and analyzed geomorphologically. Our analysis is also based on sedimentological, geochemical, palaeontological and radiometric dating data which enabled the investigation of the possible relationship between the studied swamp and the 1913 Tzivlos landslide. Sedimentological analysis showed that the current sedimentation is dominated by fine grain material and occasional coarse-grained beds. Micropalaeontological analysis indicated that the deeper layers of the core are barren, while the upper ones contain fresh water ostracods suggesting hydrodynamically a progressively more stable environment. In accordance, radiocarbon C14 and 137Cs dating showed a progressively decreasing sedimentation rate over the last fifty years. The results of this study show that the Tzivlos landslide is not the only cause for the formation of the modern swamp. Tectonic movements in the area seem to play a decisive role causing uplift and subsidence in the area near an active fault.



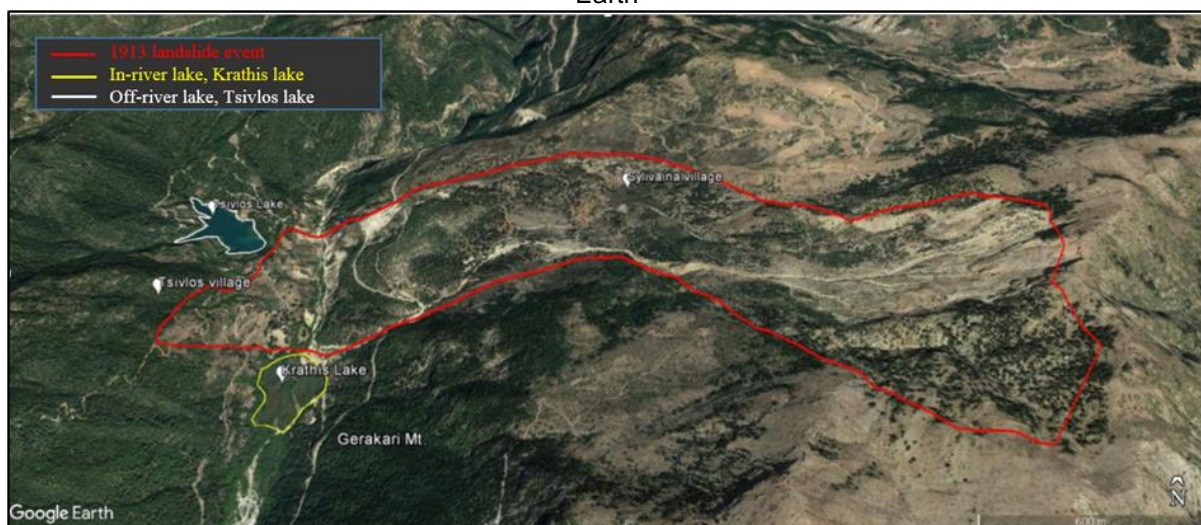
Copyright: © 2021 by the authors.
Licensee European Association of Geographers
(EUROGEO). This article is an open access article
distributed under the terms and conditions of the Creative
Commons Attribution (CC BY) license

The publication of the European Journal of Geography (EJG) is based on the European Association of Geographers' goal to make European Geography a worldwide reference and standard. Thus, the scope of the EJG is to publish original and innovative papers that will substantially improve, in a theoretical, conceptual or empirical way the quality of research, learning, teaching and applying geography, as well as in promoting the significance of geography as a discipline. Submissions are encouraged to have a European dimension. The European Journal of Geography is a peer-reviewed open access journal and is published quarterly.

1. INTRODUCTION

Large scale landslides are considered natural hazards capable in producing long term implications in the ecology and landscape evolution of a region (Schuster and Highland 2001; Korup et al. 2005; Gorp et al. 2014; Stoleriu 2015). In particular, blockage of rivers following a landslide constitutes a large-scale geomorphological process. Typical events of river blockage happen at mountainous regions with deep and narrow valleys along which a river runs (Costa and Schuster 1988; Korup 2002; Geertsema and Clague 2009). Landslides in narrow valleys many times cause the blockage of the passing river and the formation of lakes either ephemeral or permanent. These lakes except for the creation of new ecosystems and possible (eco/geo)-tourist significance (Stoleriu 2015; Salukvadze 2019) can trigger great damage and even human loss if the natural dam collapses, catastrophically (Korup 2002; Korup and Tweed 2007; Geertsema and Clague 2009; Yu-Shu et al. 2011; Gorp et al. 2014; Stoleriu 2015; Zygouri and Koukouvelas 2019). In the present study such hazardous phenomena will be researched. At present, the study area is occupied by a swamp that develops in the riverbed of Krathis River in the territory of the Chelmos-Vouraikos UNESCO Global Geopark, in north Peloponnese. This swamp constitutes the remnants of a lake formed after a big landslide (Figure 1a). The area was chosen due to the fact that a large historical landslide happened in this region, and we are trying to address the potential danger from such a landslide in the future. More specifically, in March 1913 a massive landslide wasting the Gerakari Mountain caused damages in two villages called Sylivaina and Tzivlos, impounding two lakes as well related with the Krathis river basin, one off-stream and one in-stream (Figure 1a) (Zygouri and Koukouvelas 2019). A year after the valley damming, the in-stream lake dam, called for brevity herein Krathis Lake, failed causing a massive outburst flood in the coastal zone of the Gulf of Corinth, near the present day town Akrata. The off-stream lake, called Tzivlos Lake, still remains unaffected and is considered as being in equilibrium state.

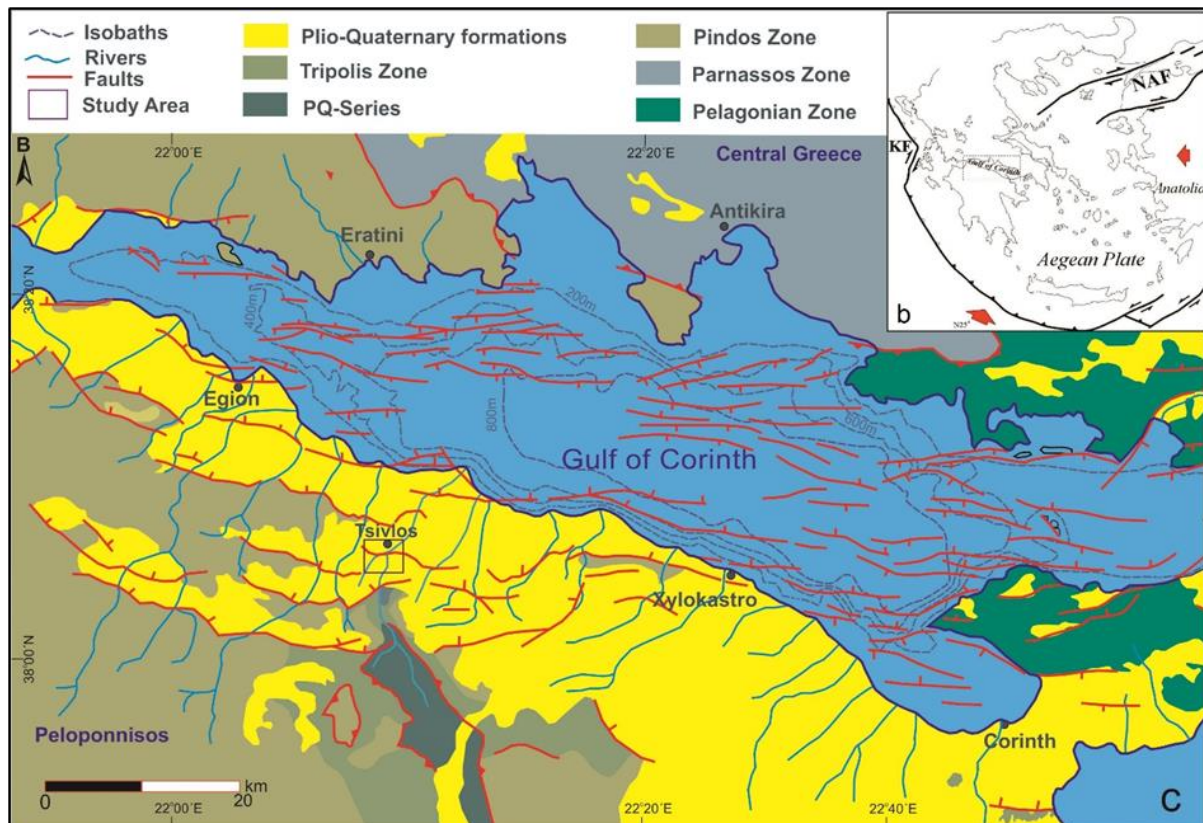
Figure 1a: the study area, with yellow line the present swamp/former Krathis Lake, with white line the Tzivlos Lake and with red color the 1913 Tzivlos landslide. Background picture derived by Google Earth



Source: Authors elaboration

The studied material from the swamp derived from a 6-m-long sediment core obtained using a percussion corer with barrel windows (Figure 1a). The core was analyzed in terms of sedimentology, micropalaeontology and ^{14}C and ^{137}Cs dating. Based on these data we will try to highlight the evolution of the Krathis Lake over the recent past and the possibility of identifying similar landslide events before 1913.

Figure 1b: the wider tectonic neighborhood of the study area, KF (Kefalonia Fault) and NAF (North Anatolian Fault). The study area is marked by the box. **Figure 1c:** local tectonic map of the study area



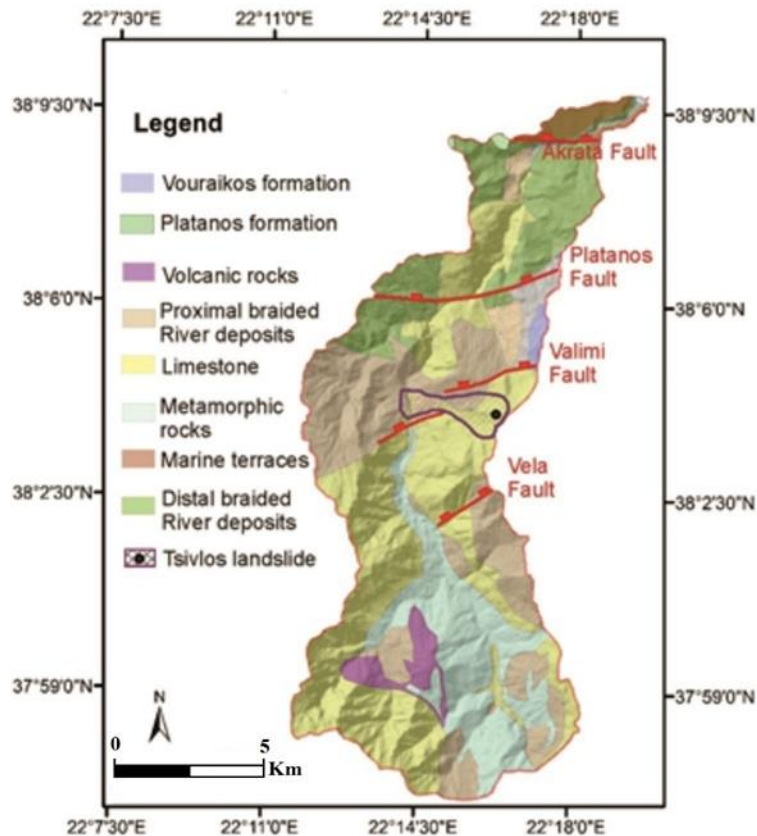
Source: Authors elaboration

2. GEOLOGICAL SETTING

The study area belongs to the geotectonic regime of the Gulf of Corinth (Figure 1b, Figure 1c). The Gulf of Corinth is a WNW-ESE directed active graben 120 km long by 30 km wide and divides the Peloponnese from the Greek mainland (Figure 1b, Figure 1c) (Doutsos and Piper 1990; Koukouvelas and Doutsos 1996; Westaway 2002; Lykousis et al. 2007; Zygouri et al. 2008). A series of WNW- and ENE- trending active faults in the area define a staircase of blocks across the north coast of the Peloponnese (Figure c) (Roberts and Koukouvelas 1996; Zygouri and Koukouvelas 2008; Hemelsdael and Ford 2016; Zygouri and Koukouvelas 2019). The graben is dominated by high subsidence rates in the north and high uplift in the south. Most of this deformation is accommodated by high angle south or north dipping normal faults (Doutsos and Piper 1990; Koukouvelas and Doutsos 1996; Westaway 2002; Lykousis et al. 2007; Zygouri et al. 2008). Strong seismicity is hosted by the graben and is concentrated across the graben's west and east ends (Koukouvelas and Doutsos 1996; Ambraseys 2009; Zygouri and Koukouvelas 2019). Because of the high rate of deformation and seismicity

in the area, several active landslides at both flanks of the graben exist (Koukouvelas et al. 1996; Gallousi and Koukouvelas 2007; Koukis et al. 2009; Lebourg et al. 2009; Chalkias et al. 2014; Polykretis et al. 2015).

Figure 2: The Krathis basin geology and major active faults modified after Zygouri and Koukouvelas (2019)



Source: Authors elaboration

The study area is located within the Krathis watershed which is extended for about 149 km² and is composed of pre-alpine and post-alpine formations (Horafas and Gkeki 2017; Zygouri and Koukouvelas 2019). Based on the separation of Greece in the Hellenides structural chain the pre-alpine formations are represented by formations that belong to the units of Tripolis, Pindos and Tyros (Koukouvelas 2019). The post-alpine sedimentary successions consist of the Vouraikos and Platanos formations and remnants of marine terraces (Figure 2) (Hemelsdael and Ford 2016; Zygouri and Koukouvelas 2019). Four main active normal faults dissect almost perpendicularly the Krathis drainage basin, namely Valimi (VF), Akrata (AF), Platanos (PF) and Vela Fault (VEF) (Zygouri et al. 2008) (Figure 2). The VF, that crosses the study area, has a length of 9 km, dipping north and forming a kilometer-wide-roll-over anticline (Groupou 2018). The Krathis River has a length of 30 km and an almost N-S orientation. It outflows into the Gulf of Corinth, where its delta extends at high depth forming a submarine steep slope (Ferentinos et al. 1988, Zygouri and Koukouvelas 2019).

3. MATERIALS AND METHODS

3.1 Sediment core

For the present study data were collected from a 6 m deep core with a diameter ranging from 50-100 mm which was drilled in the north part of the present day swamp (former Krathis Lake) (Figure 3). The geographical position and elevation of the core were determined with a differential GPS ProMark 3 Magellan. The sediment core was extracted by an Eijkelkamp portable vibrating corer with an open window barrel (Cobra TT). All extracted samples from the core were sealed with cling film and transferred to the Laboratory of Sedimentology, in the Geology Department of the University of Patras, for further analysis. In total, 135 samples were extracted from the core and 60 of them were selected for sedimentological and micropalaeontological analyses.

3.2 Sedimentology

Standard sedimentological analyses were performed including grain size analysis, and calculation of moment measures, such as mean, sorting, kurtosis and skewness, Munsell color and RGB measurements, Total Organic Carbon (TOC), Total Carbon (TC), Total Nitrogen (TN), Calcium Carbonate Content (CaCO₃) and Total Sulphur (T.S).

Sediment classification was based on grain size analysis and on Folk (1974) nomenclature. All 60 samples were fine grained, so they were analyzed with a Malvern Mastersizer 2000 and grain size distributions were calculated. GRADISTAT v.4 software (Blott and Pye, 2001) has been used to calculate grain size statistical parameters such as mean, sorting, skewness, and kurtosis. Based on the grain size analysis results, the samples are characterized as sandy silt and silt (Figure 4).

Figure 3: The sediment extracted from the sediment core of the Krathis borehole



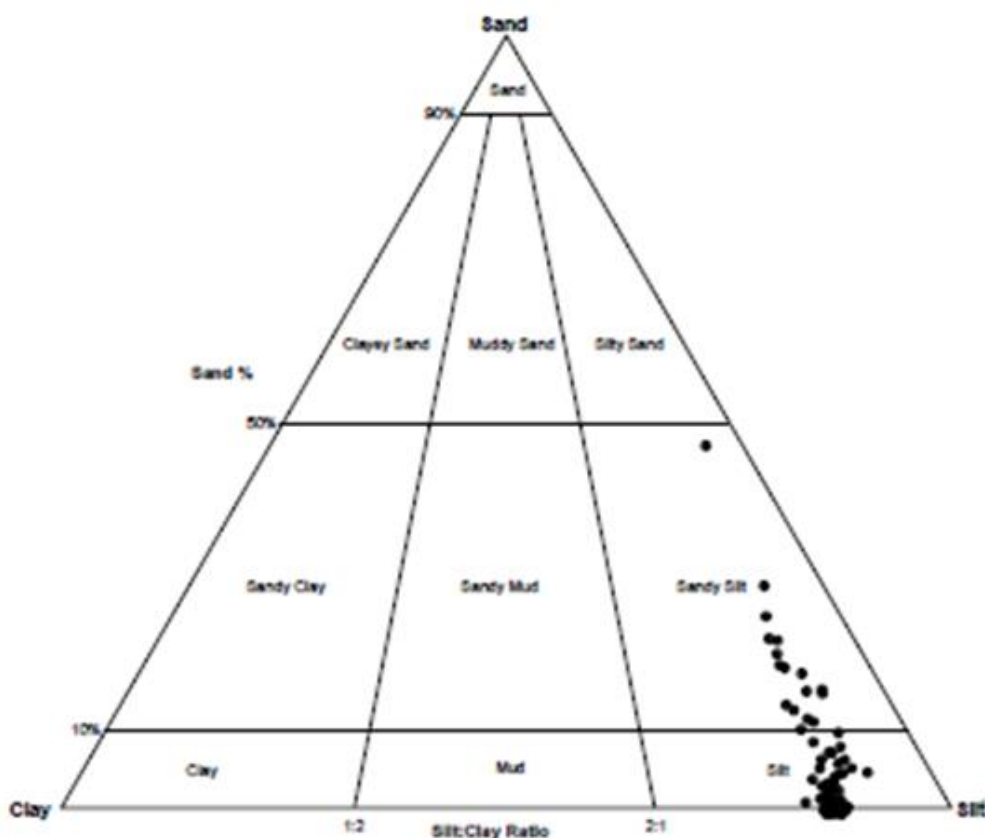
Source: Authors elaboration

Sediment colors were identified using two methods, with a Minolta CM-2002 handheld spectrophotometer based on the Munsell color chart and with RGB measurements that were taken throughout the core. Finally, the RGB results were

presented on a diagram and correlated with the sedimentological and geochemical data of the core (Figure 5).

Magnetic susceptibility was calculated throughout the core in each single cm except for the depths between 2.00 -2.42 m and 3.90-4.25 m using the Bartington Magnetic Susceptibility Meter, MS2. It is a useful parameter for the estimation of the possible source of the lake's sediment since high elevations of the magnetic susceptibility indicate greater amounts of allochthonous material in the lake (Wetzel 2001). In addition, TOC was recorded using the volumetric method of Walkley and Black (1934) and CaCO₃ using a FOG II/Digital hand-held soil calcimeter Version 2/2014 (BD INVENTIONS). CaCO₃ (%) calculation was based on measuring emitted CO₂, a modification of the method by Müller and Gastner (1971) and Jones and Kaiteris (1983). Finally T.C, T.N and T.S were calculated by using a CHNS-O EA 1108 Elemental Analyzer (Carlo Erba).

Figure 4: Sediment classification of the 60 samples based on grain size analysis and on Folk (1974) nomenclature



3.3 Chronology

The chronological framework of this study is based on two methods. For the upper part of the core the radioisotope ¹³⁷Cs was used in 35 samples collected every 3 cm across the first meter of the sediment core. For the lower part of the core two samples of wood were dated for radiocarbon age determinations at depths of 2.62 m and 4.20 m. The calculation of ¹³⁷Cs activity was carried out in the Laboratory of

Inorganic Chemistry, Radiochemistry and Physical Chemistry (Department of Chemistry, University of Patras) while Radiocarbon analyses were performed at Beta Analytic (Miami, USA). The dating results will be used for the average sediment accumulation rate which for the last 63 years was estimated using the ^{137}C results.

3.4 Micropaleontology

Sixty dried samples were picked from the sediment core for microfaunal analysis. The specimens were washed through 500 μm and 62.5 μm mesh sieves using tap water and dried. Preferably, at least 300 tests per sample (ostracods, gastropods and molluscs in this case) must be handpicked from the 62.5 μm mesh sieve sediment fraction. The core analyzed in the present study provided no sample in which 300 tests were detected and all found fauna is considered as subfossilized. Thus, since the fauna does not fulfill the qualifications to characterize them as fossils, they will be referred to, from now on, as microsubfossils. The methodology for studying microsubfossils is the same as for microfossils, meaning sorting the collected specimens, counting them and finally determining them, if possible, to the species level. Due to the small populations found in the present study, only qualitative analysis i.e. identification of the ecosystems that they represent was possible and no quantitative analysis i.e. no percentage diagrams is presented.

3.5 Geomorphology

Topographic maps and aerial photos were used for the detection of fluvial geomorphology at active environments. Such landscapes could be meanders in rivers, swamp formations, regional widening or narrowing of a river's bed, regional thick river/lake sequences, etc. In addition, as mentioned above, the average sediment accumulation rate for the last 63 years was estimated by using the ^{137}C s results. Finally, by using the software ArcMap 10.1 a digital elevation model (DEM) was created for better representation of the study area.

4. RESULTS

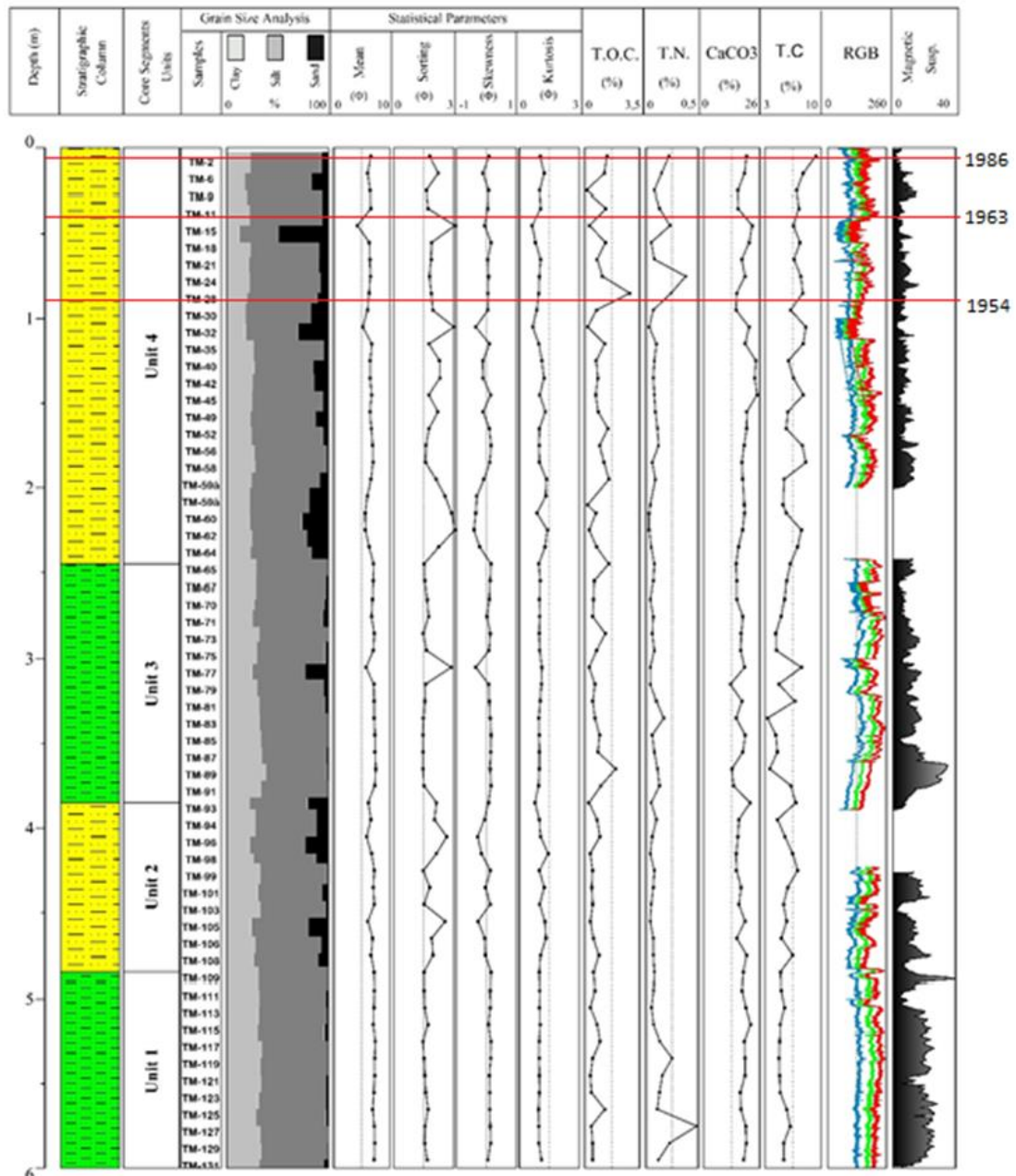
4.1 Sedimentology and Micropaleontology

Regarding the micropaleontological results the maximum specimens collected throughout the core are represented by 96 microsubfossils. Despite the small number of findings, the fact that there were both plenty of juvenile and mature ostracod valves shows that they represent in situ environments. The small number of fragmented valves possibly reveals the existence of an aquatic environment related to a stream with moderate transportation energy. Based on the sedimentological and micropaleontological results the core was divided into four units (Figure 5): Unit 1 is the lowest part of the core starting from 6.00-4.85 m, Unit 2 is the lower middle unit starting from 4.85-3.85 m, Unit 3 is the higher middle unit starting from 3.85-2.45 m and Unit 4 consists the upper part of the core starting from 2.45-0.00 m.

The lowest unit (Unit 1: 6.00-4.85 m) consists mainly of poorly sorted, olive grey fine silt. Values of sorting range between 1.453 and 1.708 Φ , with mean values ranging between 6.951 and 7.372 Φ (Figure 5). Skewness values indicate mostly a fine skewed distribution and kurtosis values show a mesokurtic distribution (Figure 5). The carbonate content ranges between 4.770 and 6.146%, TOC between 0.37 and 1.29 %, CaCO_3 between 17.1 and 21.7 %, T.N. between 0.073 and 0.486 % and finally T.S. between 0.000 and 1.174 % (Figure 5). The T.S. range was not considered in the division of the

core in units since its content was mostly close to 0.000 % throughout the core. No microfossils were detected in this unit. Based on the sedimentological data this unit possibly represents flood and swamp deposits.

Figure 5: The sedimentological, geochemical, magnetic susceptibility and RGB colors. With red line the highest picks of 137C elevations in the corresponding years and depths of the sediment core.

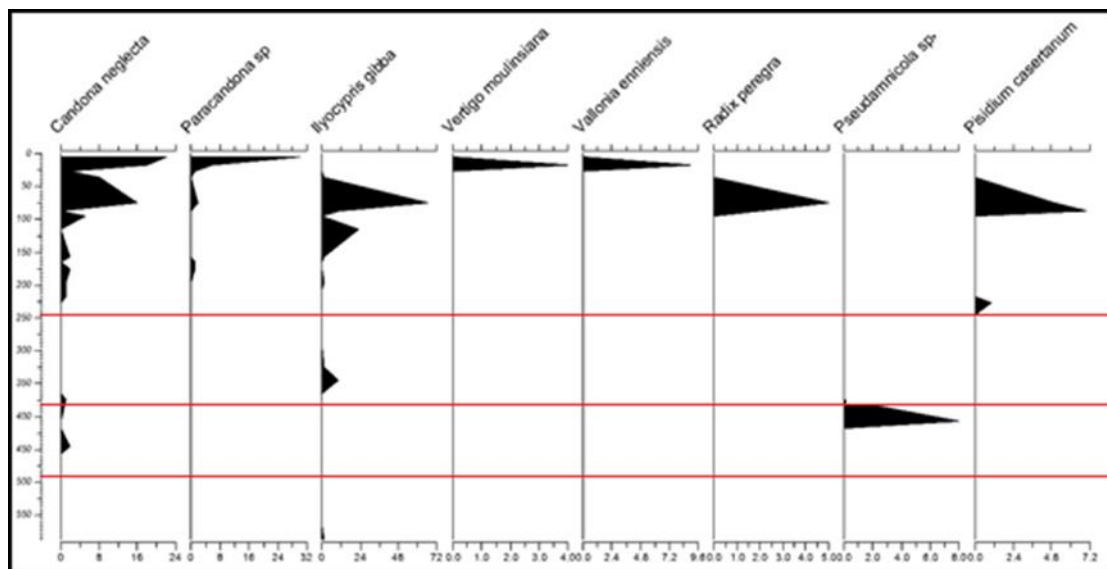


Source: Authors elaboration

The lower middle unit (Unit 2: 4.85-3.85 m) consists mostly of poorly to very poorly sorted, medium to fine silt with a small but noticeable amount of sand. Color is mostly characterized as olive grey and few appearances of grey, dark grey, brown and weak red. Values of sorting range between 1.484 and 2.644 Φ , with mean values ranging between 5.840 and 7.254 Φ (Figure 5). Skewness values indicate a fine to coarse skewed distribution, kurtosis values show a leptokurtic to platykurtic distribution

(Figure 5). The carbonate content ranges between 4.584 and 7.094%, TOC between 0.28 and 0.98%, CaCO₃ between 15.2 and 21.6%, T.N. between 0.038 and 0.097% and finally T.S. between 0.000 and 0.937 % (Figure 5). The microsubfossils detected in this unit were mostly gastropods. More specifically eight gastropods of the genus *Pseudamnicola* sp. were found and four valves of ostracods from which the two are identified as *Candona neglecta* and the other two, due to their very early stage of life, could not be determined (Figure 6). Combining the sedimentological and palaeontological data, this unit represents swamp deposits of fresh water in cool temperatures between 6-22°C (Frenzel et al 2010; Ruiz et al 2013). Furthermore, a karstic spring probably existed in the area since *Pseudamnicola* sp. lives exclusively in such environments (Szarowska et al. 2016).

Figure 6: Distribution of microsubfossils throughout the sediment core. The vertical axis showing the depth and the horizontal the abundance of each species. With red line the borders of the 4 Units.



Source: Authors elaboration

The higher middle unit (Unit 3: 3.85-2.45 m) consists mostly of poorly sorted fine silt and a small amount of medium to coarse silt, while sand is almost absent except for 3.05 m depth where an increase is noticed. Color is mostly gray and few appearances of brown, dark gray and olive gray are noticed. Values of sorting range between 1.447 and 2.859 Φ , with mean values ranging between 5.751 and 7.510 Φ (Figure 5). Skewness values indicate a fine to very coarse skewed distribution, kurtosis show mostly mesokurtic distribution and leptokurtic is observed only where coarse silt appears (Figure 5). The carbonate content ranges between 3.350 and 7.530 %, TOC between 0.29 and 1.98 %, CaCO₃ between 12.5 and 19.3 %, T.N. between 0.039 and 0.126 % and finally T.S. between 0.000 and 1.076 % (Figure 5). A small number of microsubfossils was detected all of which belong to the superfamily Cypridoidea and are represented mostly of *Ilyocypris gibba* (Figure 6). This unit also represents swamp deposits.

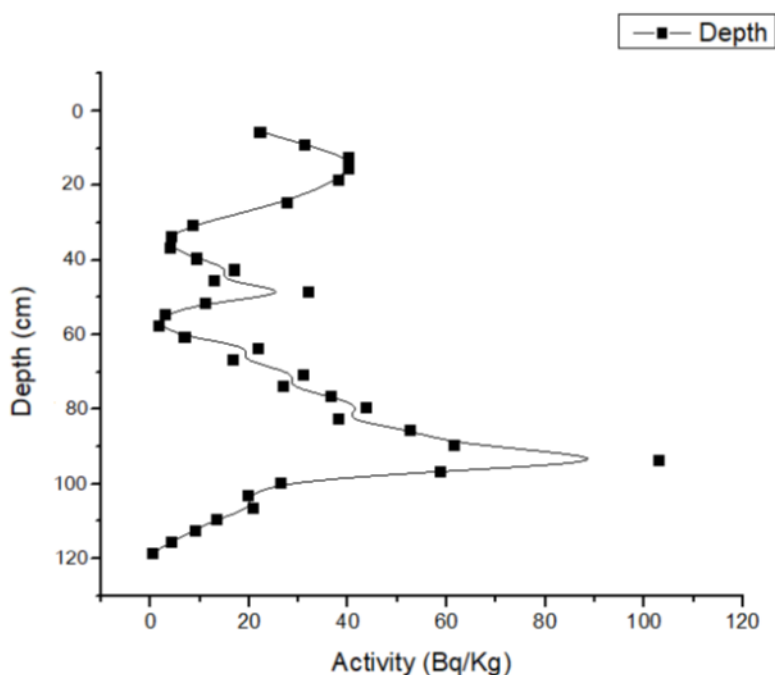
The highest unit (Unit 4: 2.45-0.00 m) consists mostly of poorly to very poorly sorted medium silt, a small amount of clay and a noticeable content of sand. Color is mostly olive gray with appearances of dark gray, gray, brown and weak red. Values of

sorting range between 1.508 and 3.045 Φ , with mean values ranging between 4.208 and 7.084 Φ (Figure 5). Skewness values range between fine and very coarse skewed distribution, kurtosis show leptokurtic to platycurtic distribution (Figure 5). The carbonate content ranges between 5.260 and 9.318%, TOC between 0.14 and 2.88 %, CaCO₃ between 15.1 and 24.7 %, T.N. between 0.027 and 0.244 % and finally T.S. between 0.000 and 0.930 % (Figure 5). This unit represents the richest unit with respect to microsubfossils since ostracodes, gastropods and bivalves are detected. Ostracods are represented by *Candona neglecta*, *Paracandona* sp. and *Ilyocypris gibba*, gastropods by *Vallonia enniensis*, *Vertigo moulinsiana* and *Radix peregra* and bivalves by *Pisidium casertanum* (Figure 6). This unit also represents swamp deposits based on the sedimentological and micropaleontological results (Frenzel et al 2010; Karanovic 2012; Ruiz et al 2013; Williams et al 2014; Bernal et al 2015). In addition, microsubfossils *Vallonia enniensis* and *Vertigo moulinsiana*, provide information for the swamp's substrate which is limestone, there were reeds and the swamp bordered with rivers banks (Beran 2006; Jankowiak and Bernard. 2013; Ksiazkiewicz-Parulska and Pawlak. 2016; Ksiazkiewicz-Parulska and Pawlak 2017). Microsubfossils also indicate a variation in water's temperature, more specifically in the depths 0.00-0.35 m and 1.57-2.27 m where *Candona neglecta* and *Paracandona* sp. dominates, the water was cooler than 0.35-1.15 m where *Ilyocypris gibba* dominates (Frenzel et al 2010; Ruiz et al 2013).

4.2 Chronology

Elevations of ¹³⁷Cs activity range between 0.5 Bq/Kg and 102.8 Bq/Kg (Figure 7a). All the years (1986, 1963 and 1954) with the highest elevations in the radioisotope ¹³⁷Cs were detected across the first meter of the sediment core. More specifically, the year 1986 (1st high elevation) is detected at 0.09 m depth, 1964 (2nd high elevation) at 0.40 m depth and 1954 (3rd high elevation) at 0.84 m depth (Figure 7a).

Figure 7a: Elevations of ¹³⁷Cs activity range.



Source: Authors elaboration

Radiocarbon ¹⁴C age determination results are reported with the units “pMC” rather than BP (Figure 7b). “pMC” stands for “percent modern carbon”. Results are reported in the pMC format when the analyzed material had more ¹⁴C than did the modern (AD 1950) reference standard. The source of this “extra” ¹⁴C in the atmosphere corresponds to the thermo-nuclear bomb testing which was on set in the 1950s. Its presence generally indicates that the material analyzed was part of a system that was respiring carbon after the on-set of the testing (AD 1950s). On occasion, the two sigma lower limits will extend into the time region before this “bomb-carbon” onset (i.e. less than 100 pMC). In those cases, there is more probability for 18th, 19th, or 20th century antiquity. In more detail the ¹⁴C results of this study are presented in Figure 7b. In addition these results suggest that the Krathis Lake during the 1950s, at least in its northern part, was a lake with a depth in the order of 4 m. This result is in accordance with the air-photos of the 1945 showing that the Krathis Lake was still existing until before its siltation in 1967 (see Figure 6 in Zygouri and Koukouvelas 2019).

Figure 7b: Radiocarbon ¹⁴C age determination results.

Depth	Measured Radiocarbon Age	Isotopes Results 0/00	Conventional Radiocarbon Age
2.62 m	113.2 +/- 0.4 pMC	d13C= - 26.0	113.4 +/- 0.4 pMC
4.20 m	103.7 +/- 0.4 pMC	d13C= - 30.4	104.8 +/- 0.4 pMC

Source: Authors elaboration

4.3 Geomorphology

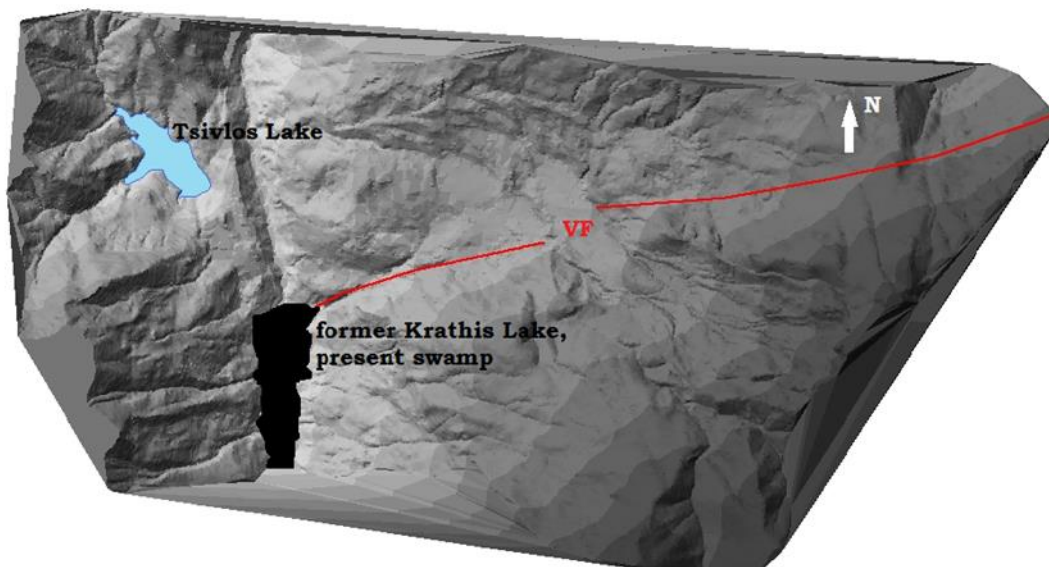
Several of the geomorphological markers that indicate active environments have been recognized in the study area such as the Krathis deep gorge (Figure 8). Another active deformation index is the river bed sinuosity of the Krathis river before its channel to cross the Valimi fault trace (Figure 9).

5. DISCUSSION

Based on the sedimentological, micropaleontological and chronological results of this study it seems that over the last 106 years in the Krathis Lake four units of fine grained sediments were accumulated, interrupted by coarser grain materials. This indicates that despite the collapse of the natural dam that caused the formation of Krathis Lake, the lake remained identifiable for about 40 years until 1950. Over this period the sedimentation rate is rapidly decreasing along with the siltation of the Lake that is progressively changing into a swamp. The existence of all three high elevations of the radioisotope ¹³⁷Cs in the sediment core indicates that the deposition of sediment continued after the year 1914 in which year the dam forming Krathis Lake collapsed. From this we conclude that Tsivlos landslide is not the only cause for the formation of the swamp. Furthermore, microsubfossils indicate changes in the lake’s temperature which also confirm that the source of the sediment in the swamp is not only the landslide but mainly later sediment accumulation from the surrounding area. Since this swamp is developed at the edge of the footwall of Valimi Fault and close to the fault trace, it is considered that the fault is active and is controlling the lake – to – swamp evolution.

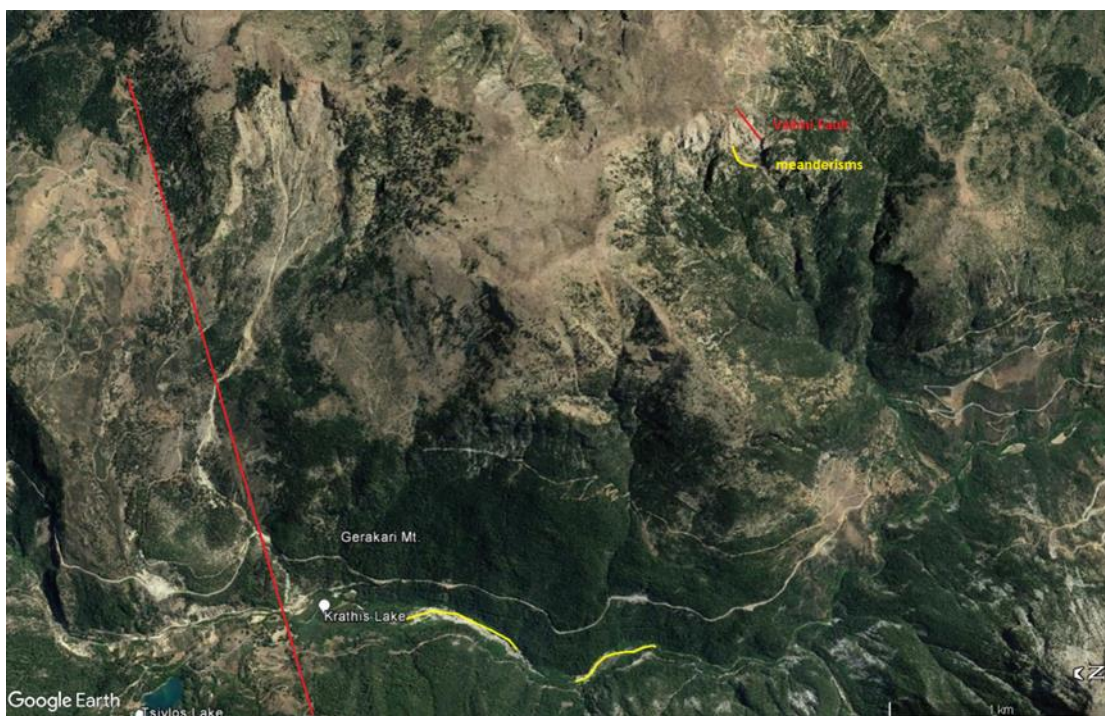
The transformation of the Krathis Lake – to – swamp along with the steepness of slopes in the area and the Krathis river bed sinuosity indicates that the swamp is accumulating sediments at high rates overcoming at present the Valimi Fault uplift rate.

Figure 8: Digital elevation model (DEM) of the study area. With red color the Valimi Fault (VF), with light blue color the Tzivlos Lake and with black color the former Krathis Lake.



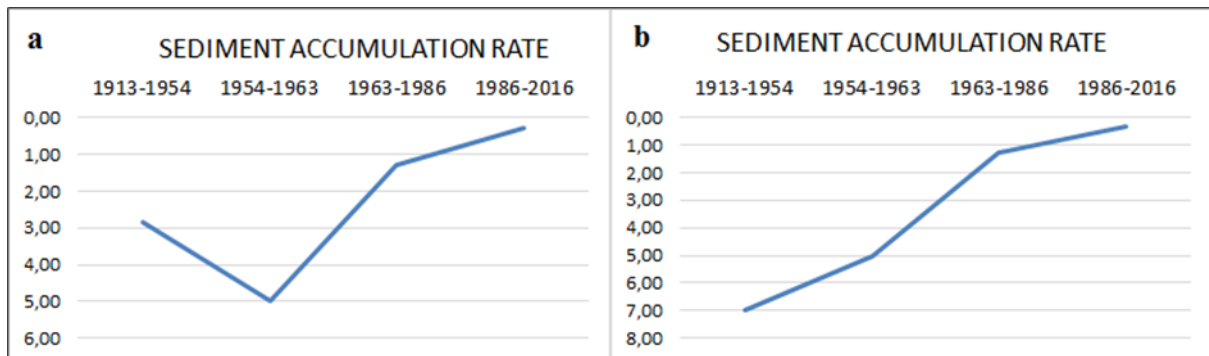
Source: Authors elaboration

Figure 9: Meanders in the Krathis River before its entering the Valimi fault trace. With red color the Valimi Fault is marked and with yellow color the meanders.



Source: Google Earth, Authors elaboration

Figure 10: Pattern of the evolution of sediment accumulation rate (cm/yr) a) for the 1st scenario: Tsvilos landslide located at 2.45 m depth of the sediment core b) for the 2nd scenario: Tsvilos landslide located at 4.85 m depth of the sediment core



Source: Authors elaboration

Findings in the Krathis swamp make unclear whether the Krathis Lake in the past accumulated the debris of the 1913 Tsvilos landslide. Based on this puzzling evidence we suggest two possible scenarios for the Tsvilos landslide event along the sediment core. First, the 1913 landslide event could be located at 2.45 m depth of the core. This scenario is based on the existence of a greater population of organisms and a continuous increase in the class of sand located at this depth. However, this scenario is impossible based on the ^{137}Cs chronological results and the radiocarbon ^{14}C age determination as well. The second scenario locates the Tsvilos landslide event at a depth greater than the 4.20 m. At this depth there is an increase in the class of sand which also agrees with the radiocarbon ^{14}C age determination results at 4.20 m depth, where the sediment corresponds to an age of 60-100 years. The 1st scenario gives us a motivo of sediment accumulation rate in the study area that would look like the one in Figure 10a which means that there might have been a time delay in the increase of sediment accumulation rate after the landslide event and then the sedimentation ratio increased rapidly. The 2nd scenario as shown in Figure 10b suggests a direct increase of the sediment accumulation rate after the landslide which is progressively decreasing until today.

6. CONCLUSIONS

Although we are not able to answer with certainty whether similar hazardous phenomena took place in the study area before 1913 as the drilling of the core has not reached the maximum depth of the lake of Krathis and the radiocarbon chronology at 4.20 m depth is highly influenced by the nuclear tests in the 50's, our results have highlighted three main conclusions.

1) The Krathis Lake formed during 1913 and remained as a lake for about four decades.

2) The sedimentation rate within this lake remained high causing the accumulation of 4.85 m of sediments in about 100 years.

3) Local meanderisms of Krathis River and the formation of the swamp indicate that the Valimi fault is active. More specifically, the Valimi fault is playing a decisive role in the formation of Lake Krathis since it was formed at the footwall of the fault. The former lake is progressively becoming a swamp under the continuous uplift and tilting to the south of the Valimi Fault footwall block.

Further investigation such as deeper drillings and at different spots in the study area are required in order to being able to reach a better understanding of the geomorphological behavior of the area such as the recurrence interval of the Tsivlos landslide.

REFERENCES

- Ambraseys, N.N. (2009). *Earthquakes in the Mediterranean and Middle East - A multidisciplinary study of seismicity up to 1900*. UK: Cambridge University Press.
- Beran, L. (2006). New records of *Vertigo moulinsiana* (Gastropoda: Vertiginidae) and notes on its distribution and habitats in the Czech Republic. *Malacologica Bohemoslovaca* 5: 14-17.
- Bespalaya, Y., I. Bolotov, O. Aksenova, A. Kondakov, I. Paltser, and M. Gofarov. Reproduction of *Pisidium casertanum* (Poli, 1791) in Arctic lake. (2015). *Royal society open science* 2(1): 1-13.
- Blott, S.J., and K. Pye. (2001). Gradistat: A grain size distribution and statistics package for the analysis of unconsolidated sediments. *Earth Surface Processes and Landforms* 26(11): 1237–1248.
- Chalkias, C., M. Ferentinou, and C. Polykretis. (2014). GIS-Based Landslide Susceptibility Mapping on the Peloponnese Peninsula, Greece. *Geosciences* 4(3): 176-190.
- Costa, J.E., and R.L. Schuster. (1988). The formation and failure of natural dams. *Geological Society of America Bulletin* 100(7): 1054–1068.
- Doutsos, T., and D.J.W. Piper. (1990). Listric faulting, sedimentation and morphological evolution of the Quaternary eastern Corinth rift, Greece: First stages of continental rifting. *Geological Society of America Bulletin* 102(6): 812-829.
- Ferentinos, G., G. Papatheodorou, and M.B. Collins. (1988). Sediment transport processes on an active submarine fault escarpment: Gulf of Corinth, Greece. *Marine Geology* 83(2): 43-61.
- Folk, R. L. (1974). *Petrology of Sedimentary Rocks*. Austin Texas: Hemphill Publishing Company.
- Frenzel, P., D., Keyser, and F.A. Viehberg. (2010). An illustrated key and (palaeo) ecological primer for Postglacial to recent Ostracoda (Crustacea) of the Baltic Sea. *Boreas* 39(3):567-575.
- Gallusi, C., and I.K. Koukouvelas. (2007). Quantifying geomorphic evolution of earthquake-triggered landslides and their relation to active normal faults. An example from the Gulf of Corinth, Greece. *Tectonophysics* 440(1): 85-104.
- Geertsema, M., and J. Clague. (2009). Natural Dams, Temporary Lakes, and Outburst Floods in Western Canada. *The First World Landslide Forum*: 211-214.
- Gorp, W., A.J.A.M. Temme, J.E.M. Baartman, and J.M. Schoorl. (2014). Landscape Evolution Modelling of naturally dammed rivers. *Earth Surface Processes Landforms* 39(12):1587-1600.
- Hemelsdael, R., and M. Ford. (2016). Relay zone evolution: a history of repeated fault propagation and linkage, central Corinth rift, Greece. *Basin Research* 28(1): 34-56.
- Horafas, D., and T. Gkeki. (2017). Applying Logistic Regression for Landslide Susceptibility Mapping. The Case Study of Krathis Watershed, North Peloponnese, Greece. *American Journal of Geographic Information System* 6(1A): 23-28.
- Jankowiak A., and R. Bernard. (2013) Coexistence or spatial segregation of some *Vertigo* species (Gastropoda: Vertiginidae) in a *Carex* rich fen in central Poland?. *Journal of Conchology* 41(3):399-406.
- Jones, G.A., and P. Kaiteris. (1983). A vacuum-gasometric technique for rapid and precise analysis of calcium carbonate in sediments and soils. *Journal of Sedimentary Research* 53(2): 655-660.
- Karanovic, I. (2012). *Recent Freshwater Ostracods of the world, Crustacea, Ostracoda, Podocopida*. Berlin: Springer-Verlag.
- Korup, O. (2002). Recent research on landslide dams – a literature review with special attention to New Zealand. *Progress in Physical Geography*: 26(2): 206-235.
- Korup, O., J. Schmidt, and M.J. McSaveney. (2005). Regional relief characteristics and denudation pattern of the western Southern Alps New Zealand. *Geomorphology* 71(3): 402-423.

- Korup, O., and F. Tweed. (2007). Ice, moraine, and landslide dams in mountainous terrain. *Quaternary Science Reviews* 26(26): 3406-3422.
- Koukis, G., N. Sabatakakis, M. Ferentinou, S. Lainas, X. Alexiadou, and A. Panagopoulos. (2009). Landslide phenomena related to major fault tectonics: rift zone of Corinth Gulf, Greece. *Bulletin of Engineering Geology and the Environment* 68(2): 215-229.
- Koukouvelas, I.K. (2019). *Geology of Greece*. Athens: Liberal Books.
- Koukouvelas, I.K., and T. Doutsos. (1996). Implications of structural segmentation during earthquakes: the 1995 Egion earthquake, Gulf of Corinth, Greece. *Journal of Structural Geology* 18(12): 1381-1388.
- Koukouvelas, I., A. Mpesiakas, E. Sokos, and T. Doutsos. (1996). The tectonic setting and earthquake ground hazards of the 1993 Pyrgos earthquake, North Peloponnese, Greece. *Journal Geological Society* 153(1): 39-49.
- Ksiazkiewicz-Parulska Z., and K. Pawlak. (2016). Rare species of micromolluscs in the city of Poznan (W. Poland) with some notes on wintering of *Vertigo moulinsiana* (Dupuy, 1849). *Folia Malacologica* 24(2): 97-101.
- Ksiazkiewicz-Parulska Z., and K. Pawlak. (2017). The influence of temperature on the hibernation patterns and activity of *Vertigo moulinsiana* (Dupuy, 1849) (Gastropoda: Pulmonata: Vertiginidae). *Turkish Journal of Zoology* 41: 370-374.
- Lebourg, T., S. El. Bedoui, and M. Hernandez. (2009). Control of slope deformations in high seismic area: Results from the Gulf of Corinth observatory site (Greece). *Engineering Geology* 108(4): 295-303.
- Lykousis, V., D. Sakellariou, I. Moretti, and H. Kaberi. (2007). Late Quaternary basin evolution of the Gulf of Corinth: Sequence stratigraphy, sedimentation, fault – slip and subsidence rates. *Tectonophysics* 440(1): 29-51.
- Müller, G., and M. Gastner. (1971). The 'Karbonat-Bombe', a simple device for the determination of carbonate content in sediment, soils, and other materials. *PANGAEA* 10: 466-469.
- Polykretis, C., M. Ferentinou, and C. Chalkias. (2015). A comparative study of landslide susceptibility mapping using landslide susceptibility index and artificial neural networks in the Krios River and Krathis River catchments (northern Peloponnese, Greece). *Bulletin of Engineering Geology and the Environment* 74(1): 27-45.
- Poulimenos, G., G. Albers, and T. Doutsos. (1989). Neotectonic evolution of the central section of the Corinth Graben. *Zeitschrift der Deutschen Geologischen Gesellschaft Band* 140:173-182.
- Roberts, G.P., and I. Koukouvelas. (1996). Structural and seismological segmentation of the Gulf of Corinth fault system: Implications for models of fault growth. *Annals of Geophysics* 39(3): 619-646.
- Rohais, S., R. Eschard, M. Ford, F. Guillocheau, and I. Moretti. (2007). Stratigraphic architecture of the Plio-Pleistocene infill of the Corinth Rift: Implications for its structural evolution. *Tectonophysics* 440(2): 5-28.
- Ruiz, F., M. Abad, A.M. Bodergat, P. Carbonel, J. Rodriguez Lazaro, M.L. Gonzalez Regalado, A. Toscano, E.X. Garcia, and J. Prenda. (2013). Freshwater ostracods as environmental tracers. *International Journal of Environmental Science and Technology* 10(5):1115-1128.
- Salukvadze G., T. Gugushvili, and J. Salukvadze. (2019). Spatial peculiarities of local tourism supply chains in high-mountainous Georgia: challenges and perspectives. *European journal of geography* 10(3):173-188.
- Schuster, R.L., and L.M Highland. (2001). Socioeconomic and environmental impacts of landslides in the western hemisphere. *U.S. Geological Survey Open-file Report*: 1-47.
- Stoleriu, O.A. (2015). Scientific and tourism value of natural dam lakes in the Carpathian mountains (Romania). Case study: Red, Cuejdel and Iezerul Savodei Lakes. *Ecology and Environmental Protection*, 14th International Multidisciplinary Scientific GeoConference SGEM 2014.
- Strom, A. (2015). *Natural River Damming: Climate-Driven or Seismically Induced Phenomena: Basics for Landslide and Seismic Hazard Assessment*. In Lollino G., D. Giordan, G.B. Crosta J. Corominas, R. Azzam, J. Wasowski, and N. Sciarra (eds). *Engineering Geology for Society and Territory* 2: 33-41

- Szarowska, M., A. Osikowski, S. Hofman, and A. Falniowski. (2015). Pseudamnicola Paulucci, 1878 (Caenogastropoda:Truncatelloidea) from the Aegean Islands: a long or short story? *Organisms diversity & evolution* 16(1): 121-139.
- Walkley, A., and I.A. Black. (1934). An examination of the Degtjareff method for determining soil organic matter and a proposed modification of the chromic acid titration method. *Soil Science* 37(1): 29-38.
- Westaway, R. (2002). The Quaternary evolution of the Gulf of Corinth, central Greece: coupling between surface processes and flow in the lower continental crust. *Tectonophysics* 348(4): 269-318.
- Wetzel, R.G. (2001). *Limnology: Lake and River Ecosystems*. 3rd ed. San Diego California: Elsevier Academic Press.
- Williams, J.D., R.S. Butler, G.L. Warren, and N.A. Johnson. (2014). *Freshwater Mussels of Florida*. Alabama: The University of Alabama Press.
- Yu-Shu, K., T. Yun-Chung, C. Kun-Ting, and S. Chjeng-Lun. (2011). Analysis of Landslide Dam Geometries. *Journal of Mountain Science* 8(4): 544-550.
- Zygouri, V., S. Verroios, S. Kokkalas, P. Xypolias, and I.K. Koukouvelas. (2008). Scaling properties within the Gulf of Corinth, Greece; comparison between offshore and onshore active faults. *Tectonophysics* 453(2): 193-210.
- Zygouri, V., and I.K. Koukouvelas. (2019). Landslides and Natural dams in the Krathis River, north Peloponnese, Greece. *Bulletin of Engineering Geology and the Environment* 78(1): 207-222